



ELSEVIER

Journal of Volcanology and Geothermal Research 101 (2000) 105–128

Journal of volcanology
and geothermal research

www.elsevier.nl/locate/jvolgeores

Seismic and acoustic observations at Mount Erebus Volcano, Ross Island, Antarctica, 1994–1998

C.A. Rowe^{a,*}, R.C. Aster^a, P.R. Kyle^a, R.R. Dibble^b, J.W. Schlue^a

^aDepartment of Earth & Environmental Science and Geophysical Research Center, New Mexico Tech, Socorro, NM, USA

^bDepartment of Geophysics, Victoria University, Wellington, New Zealand

Received 30 November 1999

Abstract

Volcanic activity at Mount Erebus is dominated by eruptive activity within a phonolitic summit lava lake. Common eruption styles range from passive degassing to Strombolian explosions, which typically occur several times daily, and occasionally in swarms of up to 900 per day. Shallow explosions, although generally the result of steady exsolution of volatiles from depth, can be triggered by surficial input of H₂O through mass wasting of rock, snow and ice from the crater walls. Broadband observations of Strombolian explosions document very-long-period (VLP) signals with strong spectral peaks near 20, 12 and 7 s, which are polarized in the vertical/radial plane. These signals precede lava lake surface explosions by ~1.5 s, are highly repeatable, and persist for up to 200 s. First motions indicate a deflationary source, with any precursory inflation being below the ~30 s passband of our instruments. Particle motions suggest a VLP source residing up to 800 m below the lava lake surface; however, this depth could be exaggerated by near-field radial tilt.

Seismic and acoustic signals associated with lava lake explosions commonly show evidence for multiple bubble bursts in corresponding complexity features resulting from varying time delays and relative sizes of superimposed bursts. A systematic decrease in seismic/acoustic ratio for smaller surface explosions suggests that either the seismic energy from the smallest, shallowest bubble bursts experiences much greater seismic attenuation than energy arising from larger events which may involve a deeper, less attenuative portion of the magma column, and/or that the shallowest layer is seismically isolated from deeper parts of a stratified magma column, which are not excited by the smallest explosions due to sharp impedance contrasts across distinct layers.

Tremor at Erebus is uncommon, with only a few isolated instances identified in five years of monitoring. Some tremor events are nearly monochromatic, and some exhibit numerous gliding harmonic spectral lines. © 2000 Elsevier Science B.V. All rights reserved.

Keywords: lava lake; explosions; tremor; seismic monitoring; acoustic monitoring; Erebus volcano

1. Introduction

Mount Erebus (Fig. 1) is the world's southernmost (approximately 78° S) active volcano, and is the most

active volcano in Antarctica (Kyle, 1994). It is remarkable in terms of its unusual phonolitic lava, its persistent Strombolian activity and its long-lived, convecting summit lava lake. Since its 1841 discovery by James Clark Ross, the volcano has probably undergone nearly uninterrupted activity dominated by frequent Strombolian explosions of gas and lava from the lake (Giggenbach et al., 1973; Kyle, 1994).

* Corresponding author. Tel.: + 1-505-835-5691; fax: + 1-505-835-6436.

E-mail address: char@dutchman.nmt.edu (C.A. Rowe).

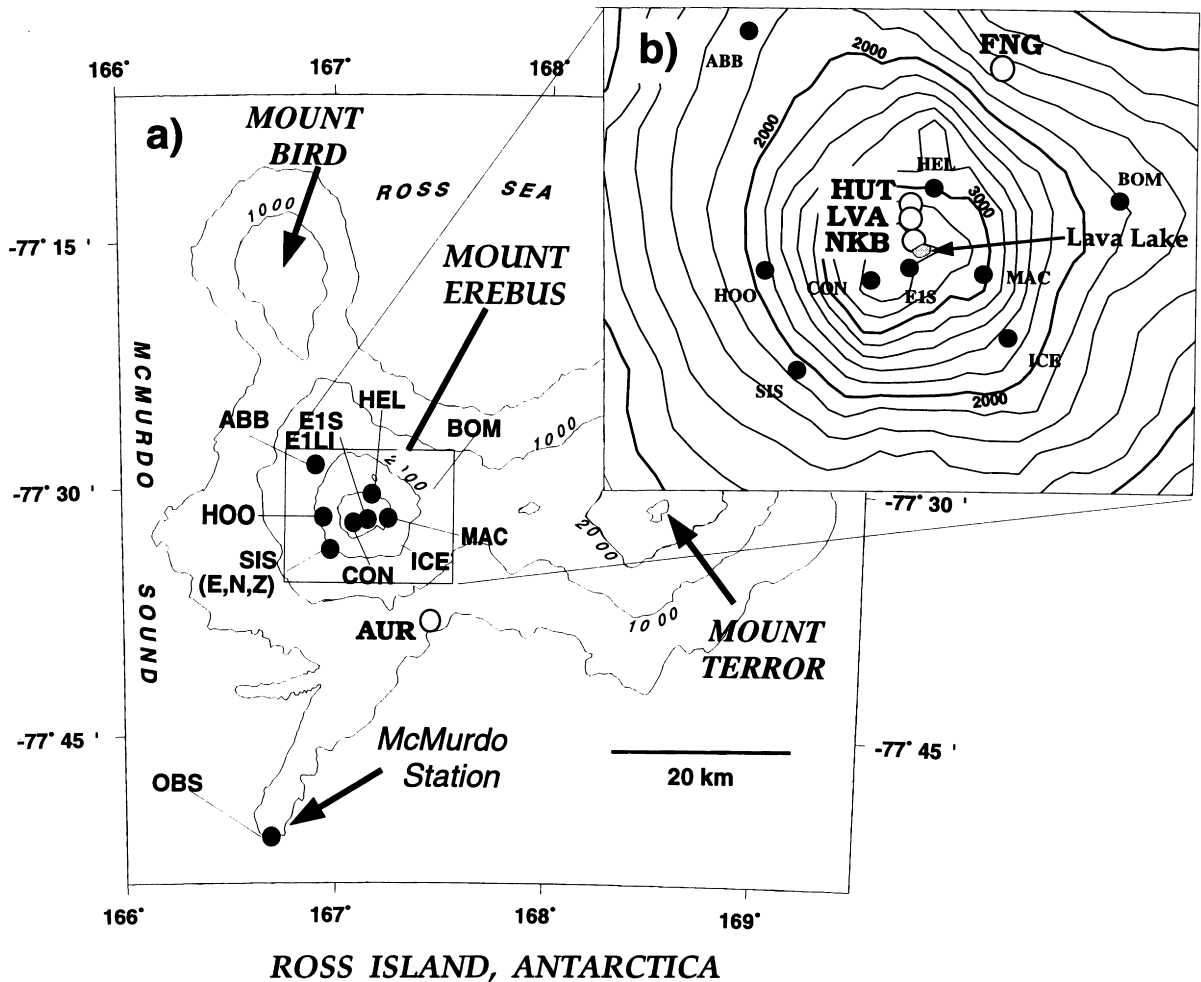


Fig. 1. Map of Ross Island, Antarctica. (a) Principal geographic features include: the active Mount Erebus; extinct volcanoes, Mounts Bird and Terror; and McMurdo Station. Mount Erebus Volcano Observatory (MEVO) short-period sensors are indicated as solid black circles. Temporary IRIS/PASSCAL sites are indicated as open circles. (b) Summit plateau area showing locations of three IRIS/PASSCAL broadband stations, NKB, LVA and HUT, as well as short-period sensor FNG. Lava lake location is indicated with an arrow.

Temporary seismic stations were deployed to monitor Erebus beginning in 1974 (Kyle et al., 1982). Between 1980 and 1990, telemetered analog networks were operated cooperatively by US, New Zealand and Japanese scientists (Kienle et al., 1981, 1982; Rowe and Kienle, 1986; Kaminuma, 1994). Additional remote monitoring included infrasonic microphones (Dibble et al., 1984; Kaminuma et al., 1985) and, from 1986 to 1990, television surveillance of the lava lake (Dibble et al., 1988, 1994a).

In 1992, the Mount Erebus Volcano Observatory (MEVO) cooperative program was established by

New Mexico Tech (NMT) and Victoria University (VUW). A six-station telemetered seismic network of 1 Hz short-period (SP), vertical component Mark Products L4C seismometers was installed on the volcano, along with an IASPEI PC-based digital data acquisition system, XDETECT (Lee, 1992), recording at McMurdo Base (Fig. 1). Data transfer protocols, developed at NMT and Los Alamos National Laboratory, were established (Skov, 1994) to facilitate daily transfer to NMT and VUW via the Internet. In subsequent years the MEVO network has expanded to ten sites on the volcano. Nine of these

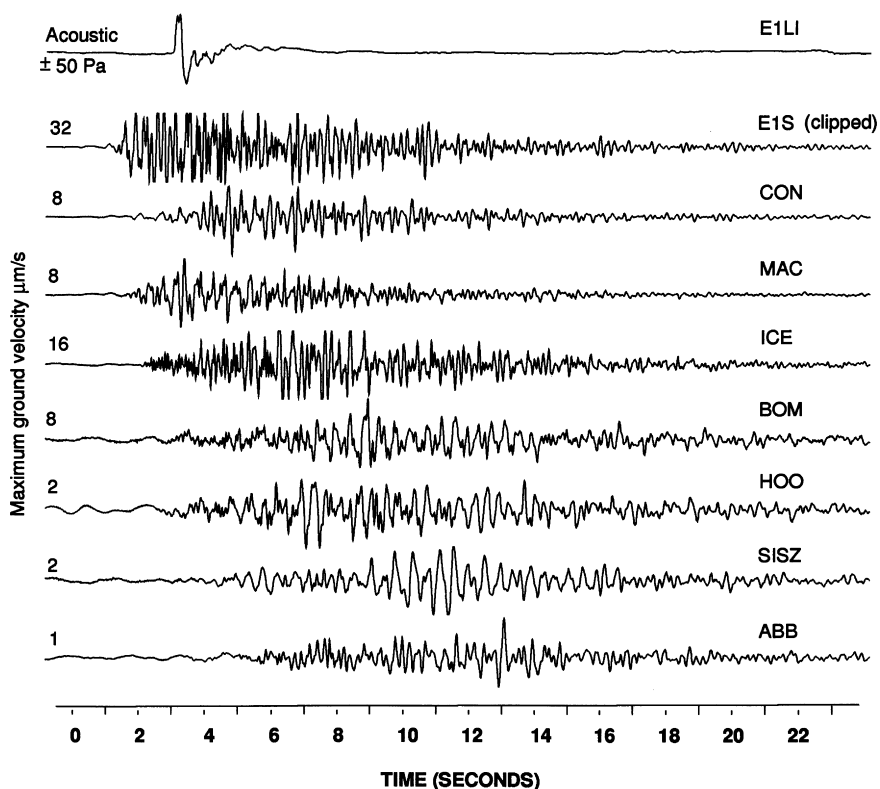


Fig. 2. Typical lava lake Strombolian explosion event at Erebus. Seismograms for eight of the MEVO permanent, short-period (1 Hz), vertical-component stations E1S, CON, MAC, ICE, BOM, HOO, SISZ and ABB are shown, as well as the acoustic sensor E1LI (top). Data are digitized at 100 s^{-1} . Note on the traces for E1S, CON and MAC, an emergent, longer-period phase can be seen about one second prior to the first, high-frequency explosion signal.

sites host short-period, vertical seismometers; and one site, Three Sisters Cones (SIS), has hosted a three-component short-period seismic station since 1996 (Fig. 1). Also in 1996, an infrasonic microphone (E1LI) was co-located with station E1S (Fig. 1) on the side crater rim. In 1997, data acquisition was expanded from the previous, event-detected, 100 sps recording to also include a seven-station 50 sps continuous data stream. Triggered and continuous data are transmitted daily to NMT and VUW for cataloguing, analysis, archiving and display on the MEVO website (<http://www.ees.nmt.edu/Geop/erebus.html>). Stations are powered by large systems of gel-cell batteries recharged by solar panels. Because of the low ($\sim 1 \text{ W}$) power consumption of the analog-telemetered stations, batteries provide sufficient capacity to maintain some network functionality throughout the Austral winter, during

which direct sunlight is unavailable for about 3.5 months. Analog helicorders at McMurdo are also employed as a secondary continuous recording system.

Three three-component Guralp CMG-3ESP broadband seismometers, with a low-frequency response corner of 0.03 Hz, were obtained from the IRIS/PASSCAL instrument pool and deployed in a near-radial line on the summit plateau during 1996–1997 (Fig. 1b) at distances of 0.7, 1.43 and 1.9 km from the lava lake (Rowe et al., 1998). Data from these instruments were recorded on a 24-bit Reftek DAS at a rate of 40 sps. Additionally, two short-period (1 Hz), three-component PASSCAL instruments, recorded at 100 sps, were positioned on the volcano's flanks to monitor icequake activity (Fig. 1). The summit plateau deployment revealed substantial very-long-period (VLP) (Chouet, 1996a), repeatable

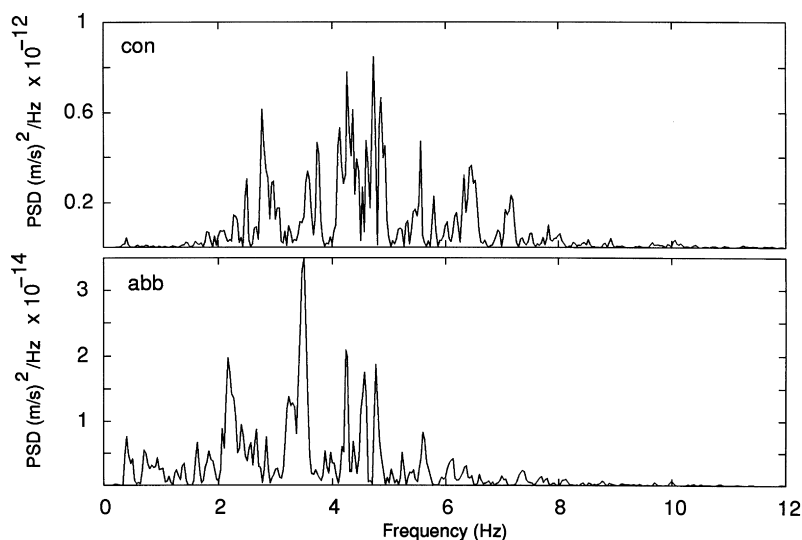


Fig. 3. Power spectral density (PSD) plots for the explosion of Fig. 2 at stations CON and ABB, 2 and 11 km, respectively, from the lava lake. Note that energy is concentrated for the most part between 2 and 8 Hz.

components of the Strombolian explosion seismic field radiating from the lava lake and conduit, dominated by energy at approximately 7, 12 and 20 s (Rowe et al., 1998).

2. Lava lake explosions

Lava lake Strombolian explosions at Erebus occur at a sustained rate of several per day, punctuated by swarms (Kaminuma, 1994; Knight et al., 1996) during which as many as 900 explosions may occur within a single day. Video observations by Dibble et al. (1988) identified four styles of emissions: strong explosions of incandescent ash and bombs from the lava lake; medium explosions of bombs but no ash; weak explosions in which an incandescent bubble domes, ruptures and folds back with few or no bombs; and eruptions of ash from vents beside the lava lake. Through many years of monitoring, the configuration of the lava lake has varied along with short-term activity levels. A three-month period of elevated Strombolian explosive activity in 1984 (Kienle et al., 1985; Rowe, 1988) buried the lake and crater floor (Dibble et al., 1994a); lower-level eruptive activity resumed when the lake reappeared in January 1985 (Kaminuma, 1994). At times the lake has crusted

over, has grown, diminished, or appeared as a convecting subsystem adjacent to a non-eruptive incandescent lava puddle in the crater floor (Dibble et al., 1994a).

2.1. Short-period seismic signals

Fig. 2 shows seismograms for a typical explosion detected by the SP network on 10 January 1998. Explosion onsets on SP records are invariably emergent, and usually show small-amplitude, lower frequency (approximately 1 Hz) precursory signals a second or two ahead of the first strong arrival. Dibble (1994) noted that such an emergent onset was consistent with the coupling characteristics expected for a conduit system with a very strong near-surface velocity gradient. Because of the limited (12-bit) dynamic range of the SP network, larger explosion signals are often clipped at the closest stations; however, spectral analysis of short-period seismic energy from smaller events shows that energy is largely confined to frequencies between 2 and 8 Hz over a range of event sizes (Knight et al., 1996). Amplitude spectra from the explosion of Fig. 2 are shown in Fig. 3 for stations CON and ABB, located 2 and 10 km, respectively, from the lava lake (Fig. 1a).

Although higher-frequency (up to 8 Hz) details of

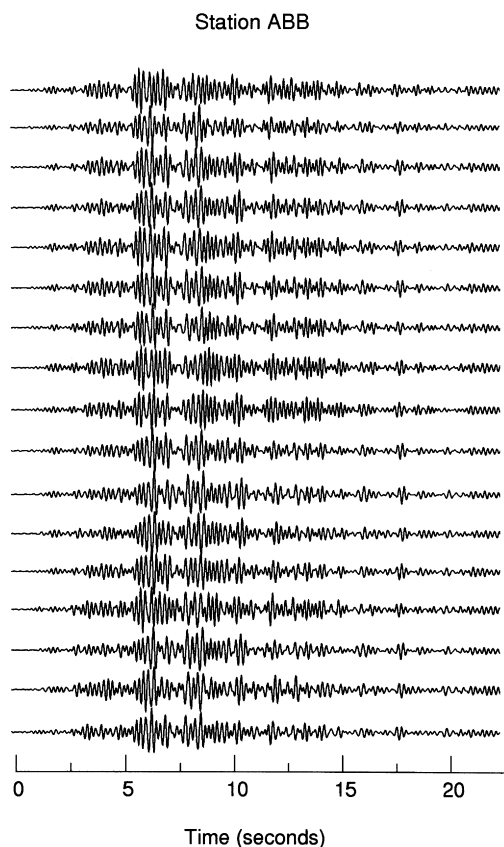


Fig. 4. Seventeen explosions recorded at ABB, 10 km from the lava lake. Traces have been bandpass filtered from 1 to 7 Hz to reduce incoherent signals. Strong repeatability of gross waveform characteristics among events is evident up to 20 s into the coda, demonstrating a repetitive source process and nearly identical raypaths arising from a small, stationary source volume consistent with the shallow lava lake.

individual event onsets vary, indicating source-time function differences, seismograms exhibit similar waveform characteristics up to frequencies of 5–6 Hz and up to 20 s into their codas, implying a maximum variation of a few hundred meters in source locations and associated consistency in raypath parameters (Dibble et al., 1984; Rowe, 1988; Dibble et al., 1994b). Such similarity is not surprising given the small (~50 m) size of the lava lake source zone. Rowe (1988) invoked this repeatability to align analog waveforms and facilitate event re-picking for the development of a working velocity model for the volcano. Dibble et al. (1988) and Dibble (1994)

utilized gross waveform similarity to stack digital explosion waveforms to enhance emergent onsets for comparing with videotaped explosion observations and for modeling velocities within the lava-lake. Time domain repeatability for explosion signals is illustrated in Fig. 4.

Since 1994, summit activity has been characterized by occasional degassing and frequent Strombolian explosions, which occur a few times per day for long periods, but which can concentrate in swarms that begin energetically and generally return over 4–5 days to background levels. Fig. 5 shows event counts taken over six-hour intervals for three lava lake explosion swarms (normalized for mean pre-swarm background seismicity level), illustrating the abrupt onset and gradual decay which often characterize typical swarm behavior (Fig. 5a and b), although activity levels may sometimes continue at a quasi-stable, elevated level for some time, as shown in Fig. 5c.

The swarm shown in Fig. 5b began on 19 December 1997, when an avalanche of debris containing rocks, snow and ice was observed to slump off the crater wall and enter the lava lake. Within seconds, numerous small bubble bursts were seen (and heard) by MEVO personnel on the crater rim (Eschenbacher, personal communication). Although the continuous digital seismic acquisition system was not operating at the time because of annual maintenance, analog helicorder records document sharply elevated explosion activity (Fig. 5b), which gradually declined to background level over the following three days. Only twenty-five of the ~630 explosions (4%) during this time were large enough to trigger the event detection acquisition system, which requires strong, impulsive signals at several stations; the vast majority of explosions were very small and presumably involved only the uppermost level of the lake. In April 1996, a four-day swarm of more than 2000 explosions was recorded, more than 900 of which occurred during the first day of the swarm (Fig. 5a). One-hundred ninety of the events triggered the event detection system (about 9%). Another distinct episode occurred during 4–8 January 1998, in which some 1150 explosions were identified in the continuous record (Fig. 5c), 69 of which (6%) were large enough to trigger the event detection system. Several other explosion swarm episodes have been noted in the

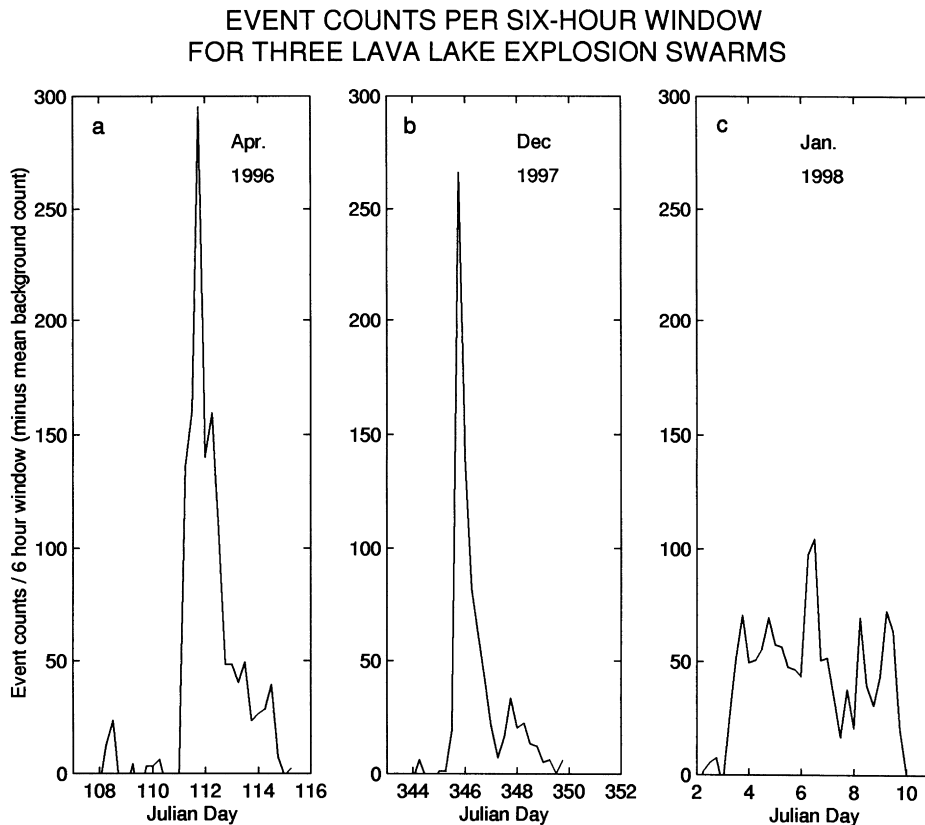


Fig. 5. Event counts at E1S for three lava lake explosion swarms, tabulated from analog helicorder records over six-hour intervals. Swarm sizes can vary significantly; note that the initial sudden increase in activity is followed by a more gradual decay period for the swarms of April 1996 (Fig. 5a) and December 1997 (Fig. 5b), while a quasi-stable sustained rate of heightened activity is exhibited for several days during the swarm of January 1998 (Fig. 5c). To limit the influence of nonvolcanic background events such as icequake activity, we have reduced the count totals by the mean six-hour seismicity level at E1S averaged over two days prior to each swarm.

two decades of intermittent monitoring of the volcano (Kaminuma, 1994; Knight et al., 1996).

Strombolian explosion behavior is likely to be predominantly controlled by the shallow volatile budget for the magmatic system, where a slight change in volatile content may result in elevated explosion activity. Usually the gas source is assumed to be exsolution of magmatic volatiles as the magma ascends from depth, although external contributions from precipitation or crater mass wasting, as in the December 1997, avalanche-related episode, can clearly be important to the explosive behavior of the lava lake system.

Cumulative explosion maximum squared seismic amplitude (proportional to source seismic energy) calculated for station ABB is shown in Fig. 6a for

364 events which were recorded by the event detection system during the period October 1997–July 1998. The overall cumulative curve is comprised of distinct pulses of activity, which correspond to the episodic swarm behavior clearly illustrated in Fig. 6b, wherein individual explosion sizes (based on maximum seismic amplitude squared at station ABB) are plotted against time. Fig. 6 illuminates behavior which may represent cycles of volatile recharge. Pulses of explosion activity initiate vigorously, beginning with larger events and gradually diminishing in size. The two gray regions in the cumulative curve of Fig. 6a, at years 98.1 and 98.5, correspond to times of extremely strong winds (year 98.1), during which background seismic noise was very high and the triggering algorithm did not

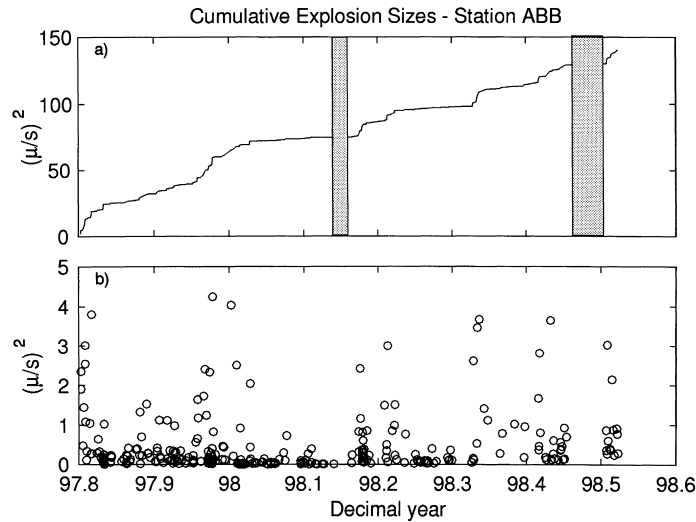


Fig. 6. Cumulative explosion sizes. (a) Cumulative curve of explosion size (maximum ground velocity squared, proportional to source seismic energy) showing that explosive volatile release proceeds in a series of pulses, which correspond to explosion “swarms” indicated in (b) The shaded areas of the cumulative curve represent times of high wind noise (near year 98.1) or network outages (near year 98.5) due to power failures in the Austral winter, which resulted in a failure of the event detection algorithm to reliably detect explosive seismicity.

capture any events, and to the reduced network sensitivity during the Austral winter (year 98.5), caused by power outages.

Sizes for digitally detected explosions between October 1996 and July 1998 are illustrated as a histogram of event counts in Fig. 7a, and as a log frequency distribution in Fig. 7b. The horizontal axes in Fig. 7a and b represent \log_{10} amplitude (m/s) (proportional to explosion seismic magnitude) measured at station ABB, chosen because its 10 km distance from the lava lake (Fig. 1a) provides the greatest number of explosion signals which are not clipped. The vertical axis in Fig. 7b shows \log_{10} of the number of events within and exceeding each “magnitude” division. Lava lake explosions arise from a source process very different from the brittle failure mechanism which causes earthquakes, and the curve shown in Fig. 7b may therefore not be expected necessarily to resemble a typical earthquake frequency/magnitude distribution. The two distinct slopes which meet at a \log_{10} amplitude of -6.5 in Fig. 7b might result from a degassing behavior which favors a median bubble burst size, as suggested from the peak in the histogram of Fig. 7a. It is also possible that the observed distribution represents the contributions of distinct populations of events, which we explore later in our

discussion of the acoustic data. Alternatively, a classical seismological interpretation of the curve in Fig. 7b suggests a power law characterization, in which we would fit a straight line to the near-linear, steeper portion of the curve, yielding a b -value of approximately 1.7. The break in slope at -6.5 is interpreted as the point below which catalog incompleteness raises questions regarding the counts of smaller events. This interpretation is consistent with comparisons of digitally detected vs. manually counted events (previously noted) which show that as few as 5% of the visible explosions which occur during swarms may be included in the digital catalog.

2.2. Broadband seismic data

Strombolian eruptions recorded by broadband (Guralp CMG-3ESP 30-s) instruments deployed during December 1996 and January 1997 (Fig. 1) revealed a significant very-long-period (VLP) (Chouet, 1996a) signal component associated with the surface eruptions, having dominant spectral peaks at ~ 20 , ~ 12 and ~ 7 and beginning approximately 1.5 s before the initial SP arrival (Rowe et al., 1998). Such signals have previously been observed in association with magmatic explosions at Stromboli

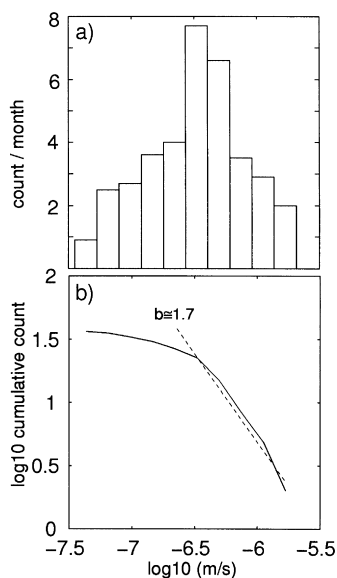


Fig. 7. Size (maximum ground velocity, m/s) distribution of 364 explosions recorded between October 1997 and July 1998. (a) histogram of explosion counts versus \log_{10} of seismic amplitude (m/s), representative of explosion seismic magnitude. (b) \log_{10} of monthly cumulative counts (for each size bin and higher) versus \log_{10} seismic amplitude (m/s). Note that sharp bend in the cumulative curve of 6b, corresponding to the peak in the histogram of 6a. This may reflect catalog incompleteness, two or more distinct populations of sources, or a preferred median size for bubble bursts. A straight line fit to the steeper portion of the curve yields a b -value of 1.7.

volcano (Neuberg et al., 1994) and phreatic explosions at Aso volcano (Kaneshima et al., 1996). Erebus VLP first motions show deflationary initiation, and are largely restricted to the vertical-radial (VR) plane (Figs. 8 and 9). Fig. 8 shows unfiltered broadband velocity records for an explosion on 15 December 1996. Fig. 9 shows a 200 s window of these records, which have been high-pass filtered at a corner of 0.01 s and integrated to ground displacement. It seems likely that the deflationary onset is preceded by a longer-period inflation (Kaneshima et al., 1996; Wassermann, 1997). Kaneshima et al. (1996) observed pre-eruption inflations at Aso with periods of more than 100 s. Such signals are outside the pass-band of our instruments and the sites are noisy at these periods, so precursory inflationary signals at such periods are not resolvable with these data. Fig. 9 also shows a 60–70 s period coherent horizontal component noise constituent which is not associated

with the explosion itself, but is due rather to tilt noise at the site. Repeatability of the VLP explosion signal is demonstrated in Fig. 10, which shows vertical displacement records from station HUT (Fig. 1b) for 15 explosions captured during the experiment. Traces were high-pass filtered at 100 s and integrated to ground displacement, then aligned on the main VLP pulse to show the high degree of repeatability among events, extending up to 100 s after the explosion. A stack of the aligned traces (top) shows a lack of any detectable inflationary pre-event signal.

The explosion VLP displacement signal (Fig. 11a, top) is centered near three clear spectral peaks (Fig. 11b). To examine the time-dependent behavior of the spectral components, we applied bandpass filters to vertical and radial components of the broadband integrated displacement record of a Strombolian explosion from 15 December 1996, for station NKB, 700 m from the lava lake (Fig. 1b). Fig. 11a shows vertical and radial components in unfiltered form, followed by the same trace pair with different bandpass filters applied to isolate the 7, 12 and 20 s period components.

VLP signals display highly elliptical retrograde particle motions (Fig. 11c) in the vertical–radial plane. The major ellipse axis points downward towards the magma conduit with an inclination increasing from ~ 33 to $\sim 45^\circ$ during the initial 25–30 s (as illustrated in the left-hand panels of Fig. 11c), followed by a more distinctly linear motion and steeper inclination (Fig. 11c, right-hand panels) of about 55° for the 7 and 20 s components, and slightly more (60°) for the 12 s constituent.

Mogi (1958) demonstrated that a spherical pressure source at depth in an elastic half-space would generate geodetic (or near-field, dynamic) displacements which are radial with respect to the source centroid. If we invoke this crude source model for the VLP source, a back-projection of the particle motion ellipse major axes suggests that its centroid resides a surprisingly deep 300 to 800 m beneath the lava lake surface; however, strain-coupled tilt, if in-phase with the seismic source (Hidaya et al., 1998), could reduce the observed horizontal seismometer acceleration (Aki and Richards, 1980) to produce an exaggerated apparent depth (Rowe et al., 1998). For example, the required amount of tilt at passband frequencies necessary to reduce the apparent horizontal acceleration by

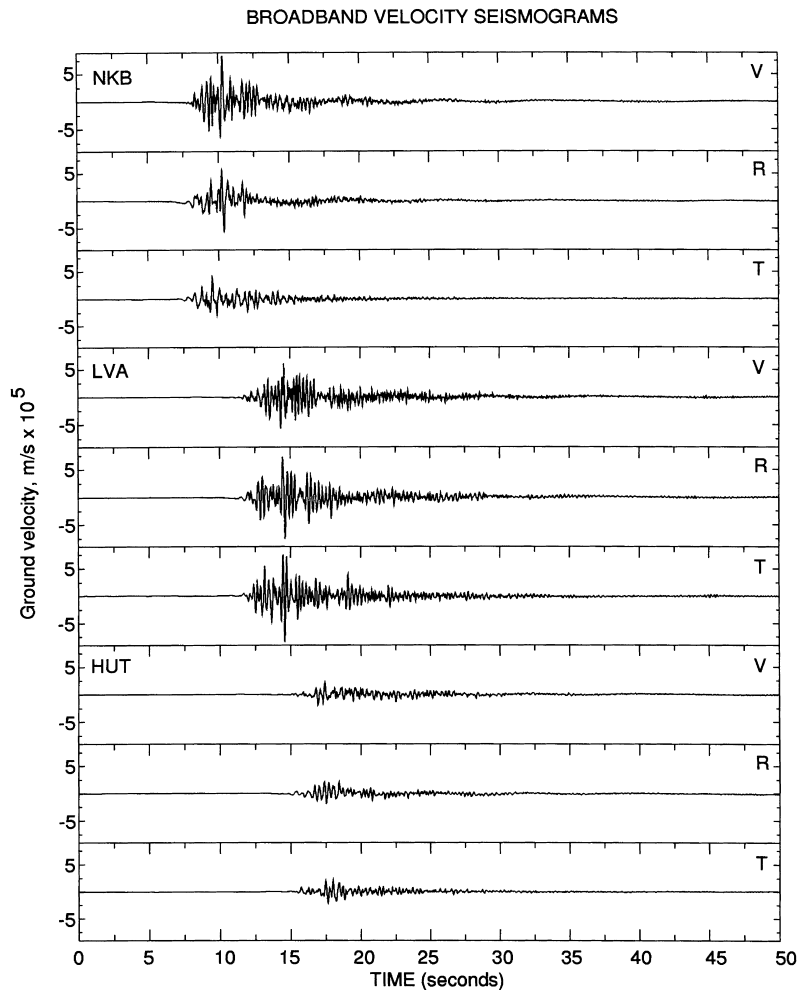


Fig. 8. Unfiltered 3-component broadband velocity seismograms of a Strombolian explosion on 15 December 1996 (after Rowe et al., 1998) recorded at NKB, LVA and HUT, deployed 0.7, 1.4 and 1.9 km, respectively, from the lava lake (Fig. 1b). A strong, very long period (VLP) component is visible on the vertical (V) and radial (R) component at all three stations and is nearly absent from the tangential (T) component. The VLP onset shows a deflationary first motion at all stations.

50% and correspondingly to increase the apparent depth is:

$$\phi \approx \frac{a}{2g}$$

where a is the apparent horizontal seismometer acceleration, g is the acceleration due to gravity and ϕ is the tilt angle. At our VLP period of 7 s, with a ground displacement amplitude of about $\pm 5 \mu\text{m}$, this yields a ground tilt angle of about $0.6 \mu\text{rad}$. Given this small value and our proximity to the VLP source, we believe

that VLP tilt could be a significant contribution to the perceived depth of source, through reducing significantly the apparent horizontal acceleration associated with lava lake explosions. Wielandt and Forbriger (1999) found that near-field radial tilt is predominant in horizontal components at Stromboli for periods ~ 50 s and longer; within the range of our VLP observations, it may contribute significantly to the horizontal signals. Future modeling of the displacement/tilt field of the volcano should confirm whether such tilts are consistent with models of the VLP source.

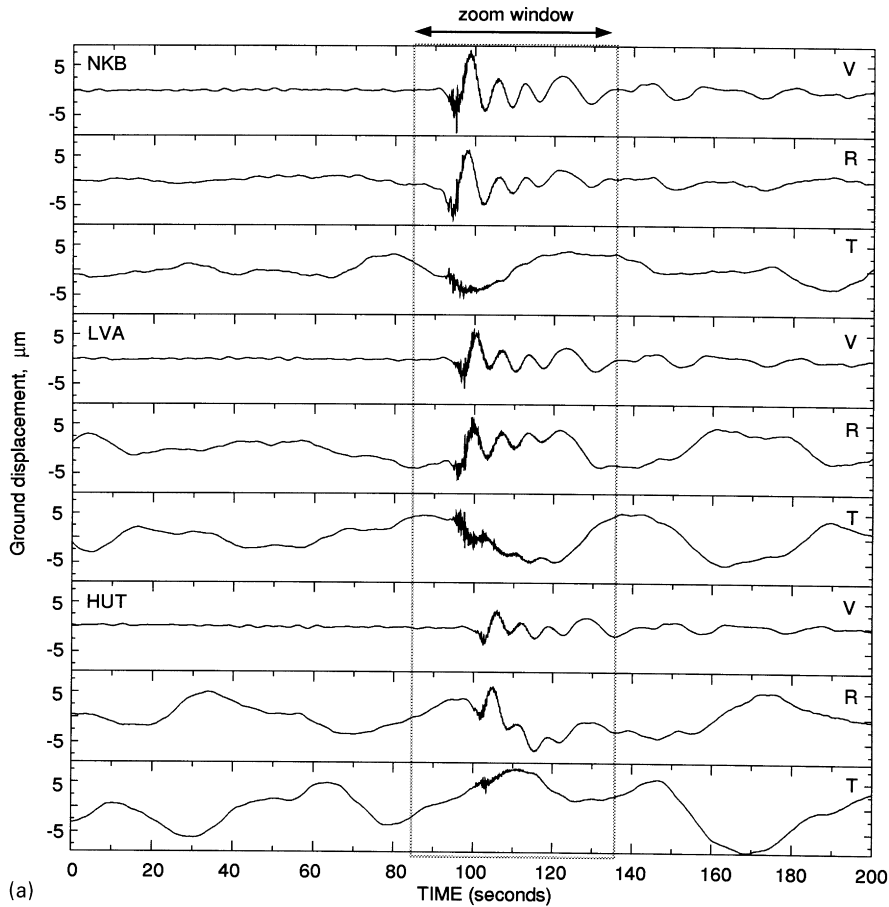


Fig. 9. (a) Broadband velocity signals from Fig. 8 high-pass filtered at a corner of 100 s and integrated to displacement. VLP signal is essentially absent from the tangential (T) components. Strong, coherent noise with a period of about 60–70 s on horizontal (R and T) components (probably tilt coupling) dominates the traces for the more distinct stations and is not associated with the explosion. (b) A close-up of the V and R traces from Fig. 9a. VLP energy precedes short-period, surface explosion-generated arrivals by ~ 1.5 s. Although some of the traces exhibit a slight upward motion prior to the first strong VLP pulse, this does not exceed the background noise (Fig. 9a) and is not uniformly observed.

Findings at other volcanoes exhibiting Strombolian activity suggest shallower source regions for the explosions, although still rather deep relative to their vent radii. Neuberg et al. (1994) estimated source depths at Stromboli to range between 100 m and 660 m below the vent, using particle motion and beam-forming methods applied to broadband array data. Through azimuth and slowness analysis of short-period array data on Stromboli (Chouet et al., 1997, 1998), these sources were estimated to reside largely at a depth of ~ 200 m beneath the crater floor. Wassermann (1997) obtained a similar apparent depth of about 200 m based on wavelet decomposition

techniques. Hagerty et al. (1997) reached similar source depth conclusions from broadband observations of explosions at Arenal volcano, Costa Rica. The explosion model proposed by Chouet et al. (1997, 1998) and supported by Hagerty et al. (1997) and Wassermann (1997) consists of a constriction in the magma conduit or ceiling of a shallow magma chamber, where exsolved volatiles collect in a foam layer, which eventually consolidates into a large gas slug that migrates to the surface and bursts.

VLP oscillations observed on Erebus following Strombolian explosions may represent resonances in the magma lake and conduit system. The excitation of

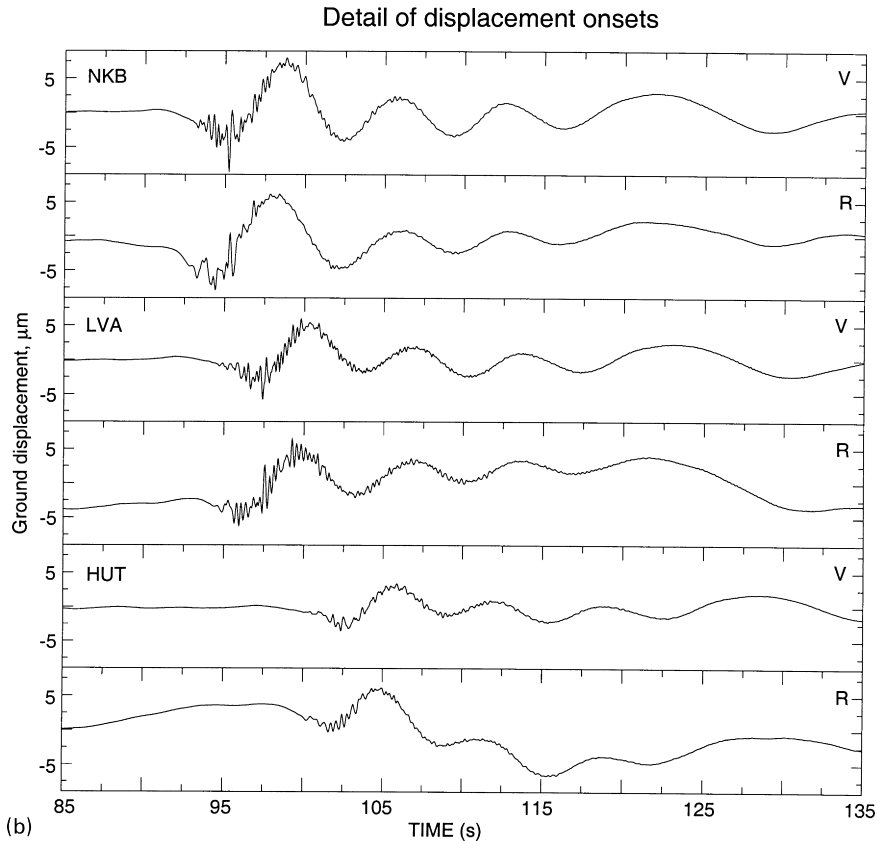


Fig. 9. (continued)

a significant resonance with periods of tens of seconds in such a narrow feeder system (~ 50 m diameter at the surface) requires very low phase velocities. Rowe et al. (1998) speculate that the gas evacuation source could excite longitudinal modes involving shear-coupled tube waves (Biot, 1952) propagating at the conduit boundary, where partial melt and a corresponding very low rigidity produce very low S-wave velocities. Alternatively, we may be observing very long period crack waves (Chouet, 1986; Ferrazzini and Aki, 1987) in a thin magma dike or still. A third possibility is that the oscillatory VLP signal may represent nonlinear, flow-forced excitation of a low-strength constriction during post-explosion readjustment of the magma lake and conduit system (Julian, 1994). Discriminating between these competing models will require both a more extensive data set and forward modeling of the seismic wavefield.

2.3. Acoustic recording

In 1996, the MEVO network was augmented with an infrasonic microphone at the volcano side-crater, co-located with station E1S (Fig. 1), 700 m from the lava lake. Availability of acoustic data greatly assists in the discrimination of lava lake explosions. Seismic and acoustic data for summit explosions show large variability in the ratio of seismic and acoustic amplitudes recorded for the 364 explosions from October 1996 to July 1998 discussed in Section 2.1. Fig. 12 shows event sizes (vertical axes) versus time (horizontal axes) for these explosions. In Fig. 12a we present the seismic amplitudes (ground velocity, in $\mu\text{m/s}$) at station ABB (the same events shown in Fig. 5), for comparison with Fig. 12b, which presents the acoustic amplitudes (pressure, Pa) for these events. Note the general amplitude correlation. Significant variability

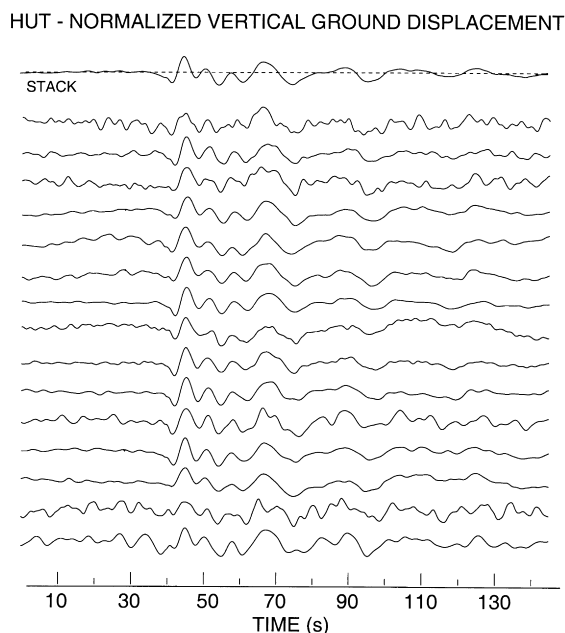


Fig. 10. Broadband explosion displacement records from station HUT, 1.9 km from the lava lake (Fig. 1b). Signals have been aligned on the main VLP pulse to illustrate the repeatability of the signal among explosions. Waveforms correlate well up to 100 s into the coda. We show fifteen Strombolian explosions recorded by station HUT during December 1996 and January 1997 and a stack (top). Displacements have been lowpass filtered to 0.5 Hz to remove SP signal components, and amplitudes have been normalized to facilitate comparison. Note that the stacked seismogram also fails to show any precursory inflation.

is apparent, however, when the two quantities are directly compared for each event in Fig. 12c, which presents the \log_{10} seismic/acoustic amplitude ratio as a function of time. This ratio exhibits a fundamentally constant level, punctuated by periods of high variability. Interestingly, the episodes of significant variation are commonly (though not always) associated with periods of swarm-type behavior.

Because we cannot isolate whether variability in the seismic/acoustic ratio is a result of changing seismic, or acoustic, coupling, unambiguous analysis of the ratio fluctuations may not be possible with these data; however, given the sensitivity of sound propagation to atmospheric wind and temperature profile conditions, we adopt the a priori assumption that seismic amplitude is a more consistent gauge of source size. Fig. 13 presents the seismic/acoustic

amplitude ratio for the aforementioned 364 events, plotted as a function of seismic amplitude (a proxy estimate of event size). A stable trend in seismic/acoustic amplitude ratio is displayed for all events of moderate to large size (the function is nearly constant above $0.4 \mu\text{m/s}$ ground velocity, as also observed for seismic and infrasonic recordings by Dibble et al. (1988)). We further note, however, a sharp decline in the ratio for smaller explosions. This break in the seismic/acoustic trend corresponds approximately to the \log_{10} amplitude = -6.5 shoulder in the seismic b -value curve (Fig. 7b), raising the possibility that, acknowledged catalog incompleteness notwithstanding, explosions could be characterized by distinct populations with independent frequency/magnitude behaviors.

Hagerty et al. (1997) and Garces et al. (1998) present evidence from seismic and acoustic observations at Arenal volcano, Costa Rica, that under quasi-stable conditions the magma conduit at Arenal may become stratified, with impedance-contrast isolated layers affecting observed seismic and infrasonic signal levels for harmonic tremor. Erebus does not exhibit persistent tremor (discussed below), so a parallel analysis is not possible, but we note that the sharp decline in seismic amplitude for smaller lava lake explosions is consistent with the shallowest portion of the lava lake exhibiting a strong seismic impedance contrast with deeper regions, either as a sharp boundary or a strong vertical gradient in elastic moduli. Dibble (1994) modeled the velocity profile of the lava lake and magma conduit, and proposed a very strong velocity gradient within the uppermost 10–60 m of the lake, based on predicted volume fraction of volatiles and magma rheology. Such a steep velocity gradient would result in substantial acoustic isolation between the upper and lower levels of the lake system. Weiss (1997) demonstrated that cumulative b -value curves for acoustic emissions can have their curvature amplitude greatly exaggerated as a result of variable attenuation characteristics. A vertical attenuation gradient can well be expected within the magma column and lava lake, as a result of the systematic changes with depth of volatile fraction and elastic moduli. An alternative or complementary explanation for the behavior Fig. 13 is thus that seismic radiation from the smallest explosions, with radii presumably restricted to the shallowest level of

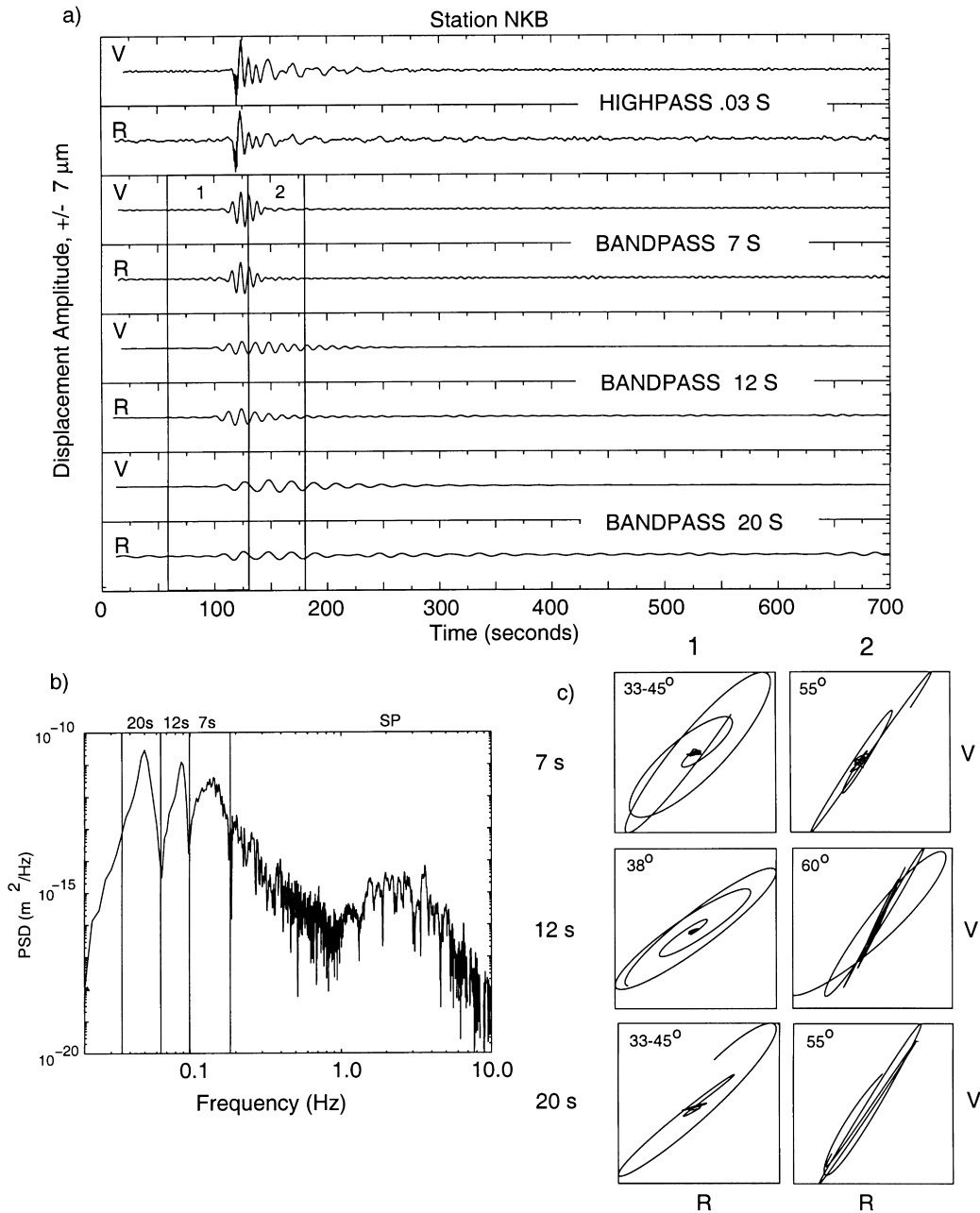


Fig. 11. (a) Vertical V and radial R component broadband displacement records of a 15 December 1996 explosion from station NKB, 700 m from the lava lake (Fig. 1b). Broadband trace pair appears at top of 8a. Below it are bandpassed records isolating the approximately 7 s, 12 s, and 20 s components of the VLP signal, obtained using two-pole Butterworth bandpass filters with corners at (0.1, 0.18), (0.065, 0.1) and (0.035, 0.065) Hz, respectively. (b) Displacement power spectral density, showing the peaks of the VLP and the distinct short-period portions of the spectrum. Vertical boxes indicate corner frequencies of the filtering applied in 8a. (c) V–R plane particle motion plots for the boxed (1 and 2) portions of three filtered trace pairs in 8a show steeply-dipping retrograde elliptical motion.

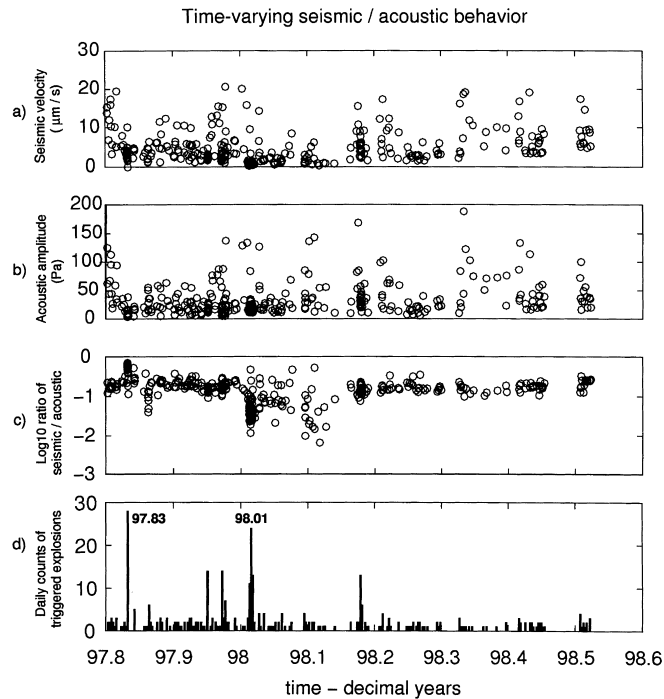


Fig. 12. Time-varying seismic and acoustic behavior of 364 lava lake explosions recorded between October 1997 and July 1998. (a) Peak seismic amplitude for individual events as a function of time. (b) Peak acoustic amplitude (pressure, Pa) for the same explosions. (c) \log_{10} ratio of seismic/acoustic size. Note a generally stable ratio trend, punctuated by periods of strong variation. (d) Daily triggered explosion counts for the data set shown in (a), (b) and (c). The swarms occurring at approximately years 97.83 and 98.01 indicated by strong peaks in (d), are temporally related to two of the periods of seismic/acoustic amplitude fluctuation in (c), suggesting that ratio fluctuations are associated with swarm-type behavior.

the system, is more strongly attenuated than seismic radiation from larger explosions.

Fig. 14a shows a typical acoustic signature associated with a bubble burst in the summit lava lake. Fig. 14b shows the amplitude spectrum for this signal; note the corner frequency at approximately 3 Hz. To first order, the frequency characteristics of acoustic records are consistent among explosions over about two orders of magnitude in event size. In Fig. 15 we show the normalized acoustic spectra (\log_{10} PSD) for 99 explosions, displayed as a surface whose horizontal axis represents frequency and whose vertical axis represents individual explosions, sorted as a function of increasing mean value of their spectra. The spectra have been amplitude-normalized so that the overall shapes may be compared. Note a relatively consistent corner for all events at around 3 Hz, irrespective of the absolute (unscaled) amplitude (there is no systematic trend in the frequency of this corner as we move to

larger events), and the common spectral peaks and troughs among events, manifested as vertical banding on the surface. These similarities show that the dominant spectral shape of the acoustic signal is independent of the source size and may reflect the acoustic properties of the lake or crater (path effects), rather than acoustic properties of the explosion sources themselves. Dibble et al. (1984) interpreted analog infrasonic signals as having dominant periods proportional to source (bubble) diameter; however, we see no evidence for this correspondence dominating the current data. To verify that the constant corner frequency of ~ 3 Hz is not an instrumental artifact, we stacked the PSD for five-minute continuous microphone recordings over a two-hour period during moderately noisy conditions so that we might examine the instrument response to a random and broadband source. This PSD is shown in Fig. 16. The instrument response drops off smoothly between

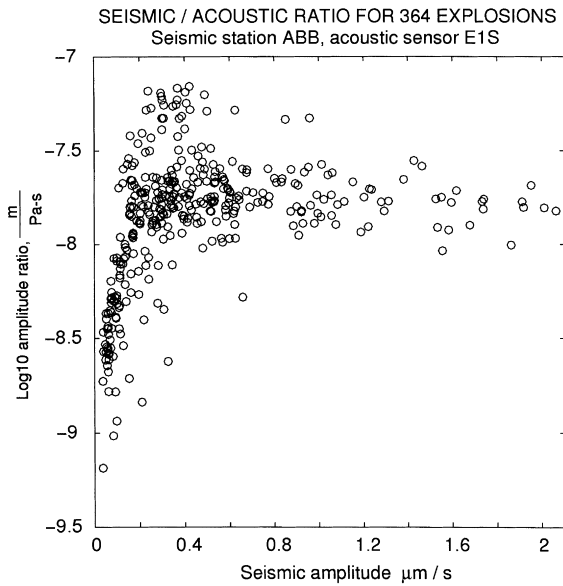


Fig. 13. The \log_{10} seismic/acoustic ratio plotted as a function of maximum seismic amplitude. The seismic/acoustic ratio appears fairly constant for events of maximum seismic amplitude greater than about $0.3 \mu\text{m/s}$; below this size a sharp decrease in the ratio correlates with diminishing event size.

~ 0.03 and ~ 10 Hz, as a function of about ω^{-2} , with no slope change near 3 Hz.

As noted earlier, gross seismic waveform similarities among explosions have been invoked for consistent event location and velocity modeling (Dibble, 1994; Dibble et al., 1988; Rowe, 1988); however, details of signal onset show a range of variability suggesting variation in source-time functions. Such variations should manifest themselves both among seismic and acoustic recordings, and may be more easily investigated with acoustic data because of the much simpler Green's function through the atmosphere. A comparison of individual explosion acoustic records reveals variability in the waveform details consistent with superposition of multiple, discrete pulses. As noted by Dibble et al. (1984), events with acoustic impulses exhibiting complexity also demonstrate a parallel degree of complexity in their seismic onsets. Fig. 17 illustrates representative acoustic (Fig. 17a) and seismic (Fig. 17b) recordings for a suite of explosion events recorded at acoustic sensor E1LI and co-located seismometer E1S (Fig. 1) between October 1997 and July 1998.

We explore the question of superimposed pulses by empirically summing two identical, simple (lacking discernible sub-events) Green's functions from the

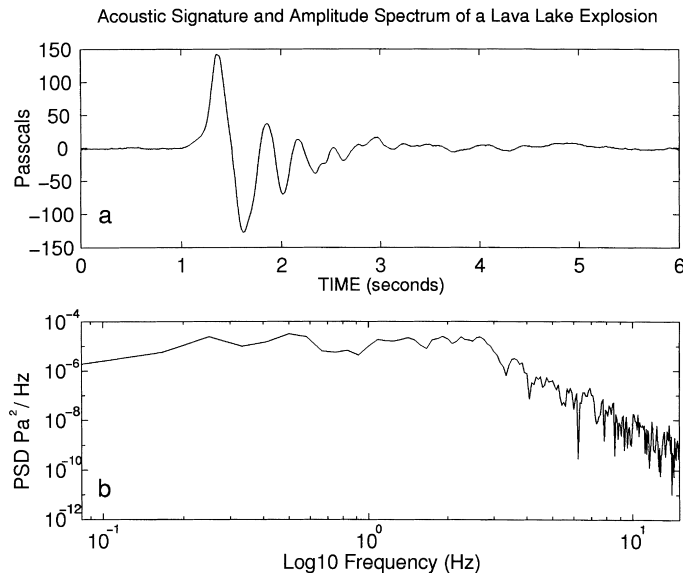


Fig. 14. Typical acoustic signal from a single lava-lake bubble burst. (a) Waveform exhibits a simple impulse whose oscillations decay exponentially over about 4 s. (b) PSD for the signal of 14a, showing a corner frequency near 3 Hz.

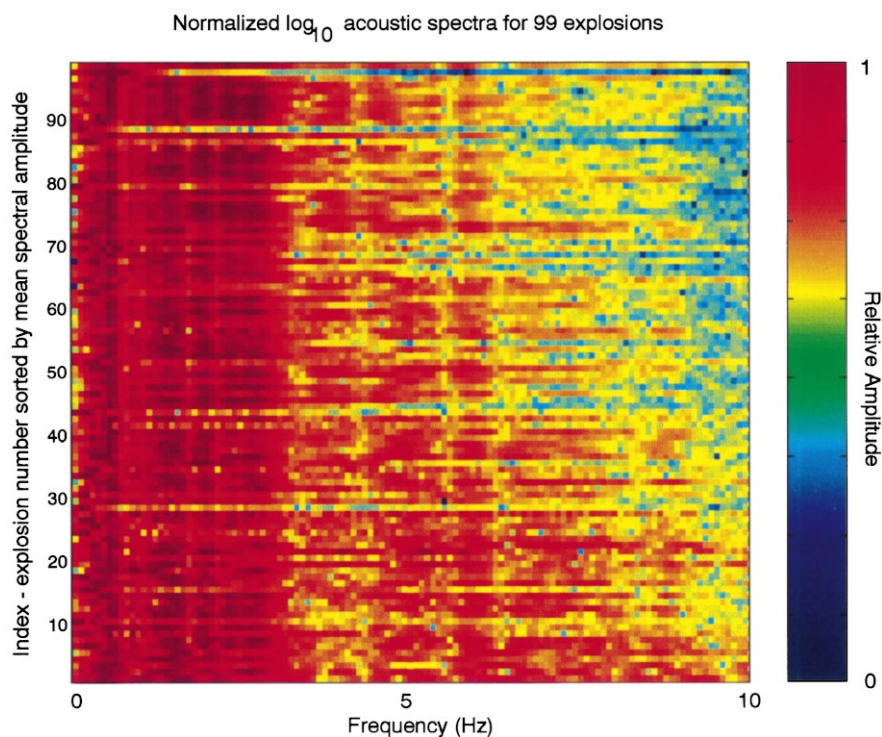


Fig. 15. Acoustic spectra for 99 lava lake explosions, ranging between 2 and 152 Pa in maximum acoustic amplitude. Events are sorted so that mean PSD amplitude increases monotonically from the bottom of the plot; frequency is plotted on the horizontal axis. Spectra have been normalized by their mean values to facilitate a comparison of spectral shape. The consistent spectral corner at 3 Hz can be seen across the range of event sizes, as can other consistent spectral peaks (manifested as vertical banding on the plot). This implies that dominant spectral characteristics of the acoustic signal are essentially independent of event size and thus probably reflect the acoustic characteristics of the lava lake or crater (path effects), rather than consistent source features.

acoustic data. A range of delay times and amplitude ratios is applied, and the resulting shifted and scaled signals are summed to produce the suite of waveforms tabulated in Fig. 18a. Superposition of sources with lags of between 0.15 and 0.3 s provides a good empirical fit to the observed acoustic signatures for 70% of the explosions examined (Fig. 18b). The best matches to recorded signals often occur when the delayed pulse has an amplitude equal to or greater than that of the first pulse. We therefore conclude that the multi-pulse (complex) signals are not the result of multipathing, but arise rather from two (or more) individual sources, separated somewhat in time and perhaps space; however, presently we are unable to resolve whether the signals arise from two spatially separated sources or a single, sputtering type of burst.

3. Volcanic tremor

Almost all active volcanoes exhibit tremor (McNutt, 1994). Many, such as Stromboli (Chouet et al., 1997), Kilauea (Aki, 1981), Pavlof (Benoit and McNutt, 1997) and Arenal (Hagerty et al., 1997; Garces et al., 1998) routinely exhibit sustained harmonic tremor, characterized by stable spectral peaks in an extended signal (McNutt, 1994; Chouet, 1996b; Benoit and McNutt, 1997; Hagerty et al., 1997; Chouet et al., 1997, 1998). Harmonic tremor has been successfully modelled as a sustained pressured oscillation of fluid-filled cavities or conduits (Chouet, 1981, 1985; Julian, 1994), or as continuous bursting of small bubbles at the top of a magma column (Ripepe et al., 1996).

Erebus has exhibited surprisingly few instances of

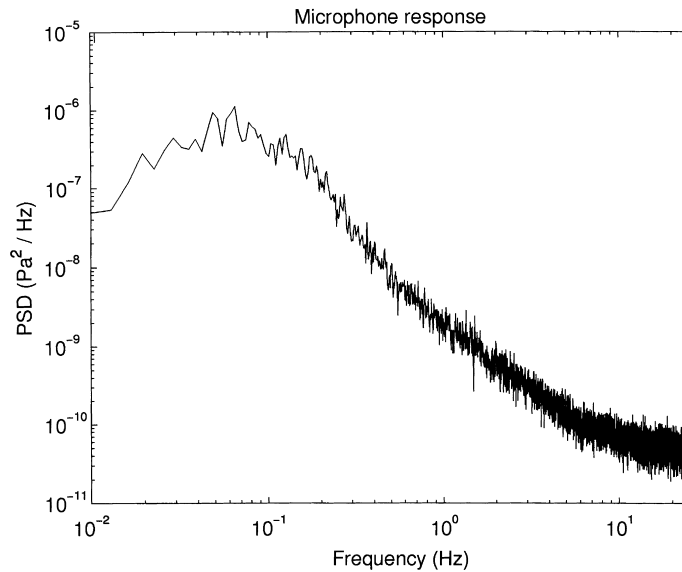


Fig. 16. Stacked PSD for wind noise at acoustic sensor E1LI. Two hours of moderately noisy acoustic signal (digitized at 50 s^{-1}) were used to show the microphone response to a broadband excitation. Successive five-minute segment spectra were calculated, then the resulting spectra were averaged. Note the smooth falloff between ~ 0.03 and ~ 10 Hz, as a function of about ω^{-2} . No pronounced corner is exhibited near 3 Hz, indicating that the corner frequency seen in explosion acoustic records (Fig. 15) is not an instrumental response artifact.

harmonic tremor, despite its ongoing activity. Tremor was first observed on analog records during a probable dike injection episode beneath Abbott Peak (Kienle et al., 1983; Ueki et al., 1984; Knight et al., 1996; Rowe, 1998) in October, 1982. A brief episode, lasting ~ 20 min, was captured by the MEVO triggered digital system in January, 1995 (Knight et al., 1996). Fig. 19a illustrates 30 s of recording at all operating stations, and Fig. 19b illustrates 180 s of seismic signal and associated spectrogram, recorded at station HOO. This tremor has a maximum amplitude at central stations E1S and CON of about $\pm 5 \mu\text{m/s}$, and a sharp spectral peak at ~ 2.5 Hz, with few if any higher peaks. The frequency dropped slightly after a few minutes, a behavior referred to as “gliding,” a gradual, proportional frequency shifting of spectral peaks (Hagerty et al., 1997; Garces et al., 1998). The signal was easily seen at station MCM (since renamed OBS, see Fig. 1), ~ 37 km away at McMurdo, indicating that it was caused by a deep, energetic magmatic event.

Routine continuous, digital recording on Erebus and other volcanoes has improved the recovery of emergent, sustained signals such as tremor, which

would be unlikely to be recorded on a triggered system (Rowe and Davies, 1990; Tytgat et al., 1992). Brief (10–20 min) episodes of very low amplitude harmonic tremor occurred at Erebus on 4 and 5 April 1998, and 2 August 1998. These were identified through scanning of pseudo-helicorder plots (Stephens, 1996), generated from 24-hour digital data streams. As with the January 1995 episode, the signals were largely monochromatic although the April 1998 tremor exhibited one distinct harmonic.

On 11 May 1998, a more complex episode of tremor occurred. A 60 s sample of the 50 sps continuous MEVO network recording is shown in Fig. 20a. This instance of tremor differs markedly from the 1995 and the April and August 1998 episodes, in that it exhibits at least twelve strong spectral peaks (Fig. 20b). Amplitudes overall are much smaller than the 1995 tremor, with peak amplitudes at station E1S (Fig. 1) of only $\sim 0.6 \mu\text{m/s}$. Largest overall amplitudes occur at station E1S, nearest the central conduit and lava lake. Gliding of approximately one spectral line spacing (0.5 Hz) is evident (Fig. 19b). Chouet (1996b) proposed that gliding represents an alteration of the physical dimensions

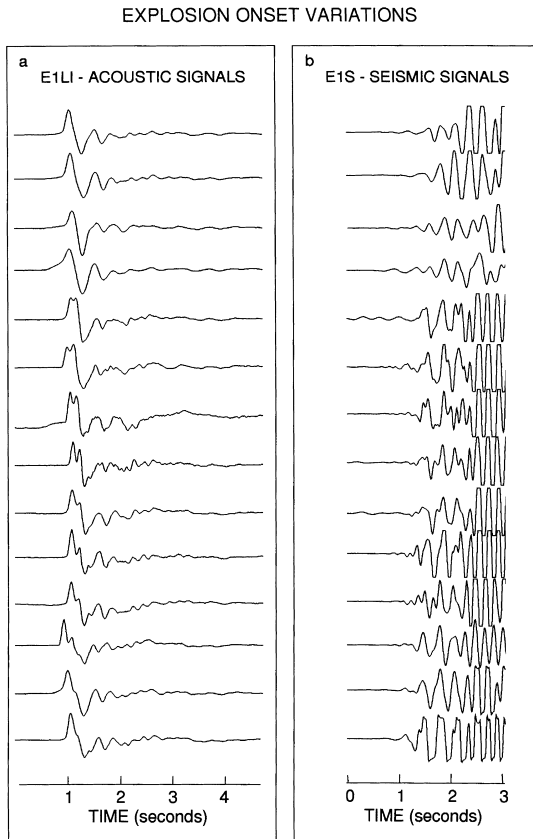


Fig. 17. (a) Fourteen E1LI acoustic recordings of lava lake explosions, illustrating a suite of subevent variability. (b) Onsets of corresponding seismic signatures for the fourteen explosions recorded at station E1S, co-located with the acoustic sensor E1LI (Fig. 1a), illuminating parallel variability in seismic signal. These variations in both seismic and acoustic waveforms among events are indicative of source sub-events.

of the resonant chamber which produces the tremor (widening or stoping) while Hagerty et al. (1997) and Garces et al. (1998) alternatively suggest that it reflects either a change in the acoustic properties of the melt, i.e. evacuation or introduction of volatiles, or an extension of an acoustically isolated layer within the magma conduit through chemical/volatile adjustments to layer boundaries. Another such episode of similar amplitude was noted on 2 September 1998, which was noteworthy in that it continued intermittently for nearly two hours and alternated between complex, polychromatic and nearly monochromatic signal.

There is no definitive acoustic signal associated

with the 1998 Erebus tremor episodes (the acoustic sensor had not been installed in 1995), despite relatively quiet background levels. Garces et al. (1998) invoke acoustic decoupling between lower, volatile-poor magma and an upper frothy layer as an explanation for a frequent lack of acoustic signals at Arenal volcano during episodes of strong harmonic tremor. Immediately following explosions, however, tremor at Arenal exhibits an acoustic signature, which Garces et al. (1998) interpret as a manifestation of disruption of the normally stratified magma column, mixing the separate layers and destroying the hypothesized acoustic isolation. We acknowledge this as a viable explanation, but we have insufficient tremor data in close association with large explosions to draw any such support for acoustic isolation of tremor in the Erebus conduit system. Tremor amplitude is less attenuated with distance by a factor of ~ 5 compared to Strombolian explosion signals from the summit lava lake containing comparable frequencies, suggesting a comparatively deep source and raypaths in the higher- Q , deeper regions of the volcano.

4. Summary

Volcanic seismic activity at Erebus is dominated by frequent Strombolian explosions within the summit lava lake. Explosions occur several times daily, with events often concentrating in 4–5 day pulses of swarm activity. Explosions repeatedly originate within a small volume, consistent with the shallowest portion of the ~ 50 m diameter lava lake, as shown by a waveform similarity due to nearly identical ray paths among events, which persists for tens of seconds into event codas at frequencies up to several Hz. Explosion size distribution follows an approximately power law distribution with a b -value of about 1.7. A corner in the cumulative distribution curve may be due to catalog incompleteness, or to distinct source population distributions or a preferred median bubble size.

Broadband observations of Erebus Strombolian eruption activity show a repeatable, very-long-period (VLP) signal, dominated by energy near 7, 12 and 20 s, with a deflationary onset preceding large lava lake bursts by ~ 1.5 s. The VLP signals persist for

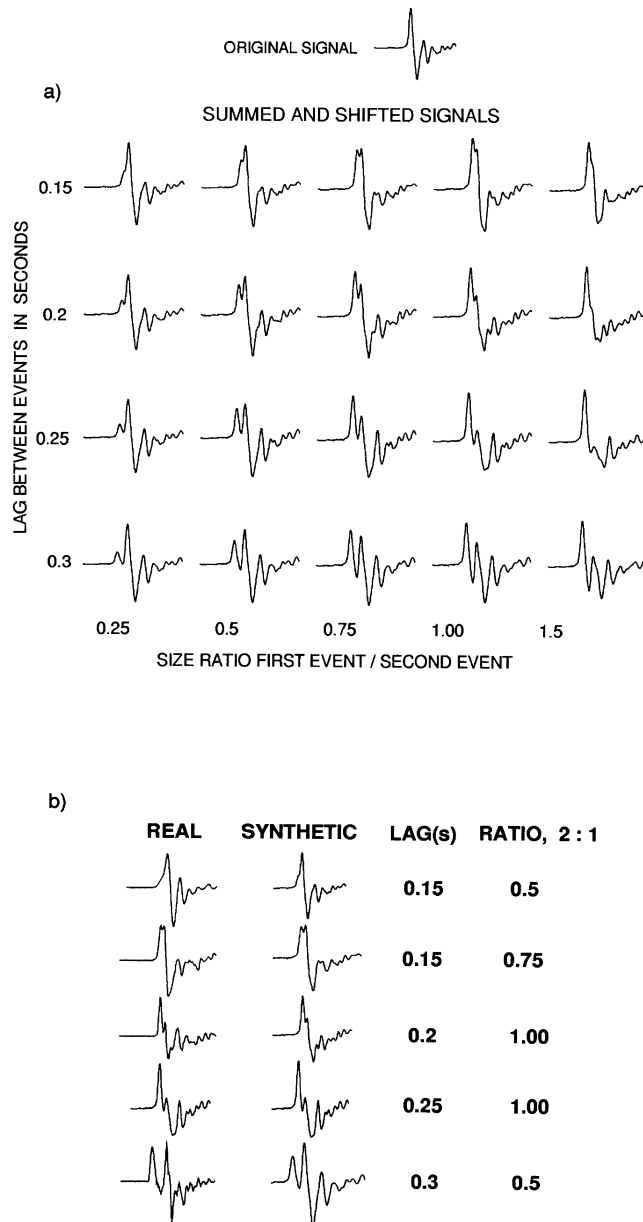


Fig. 18. (a) Synthetic acoustic signals produced by superimposing pairs of simple, identical acoustic Green's functions with a range of amplitude ratios and time lags. The resulting suite of synthetic acoustic signals closely mimic actual acoustic signal variants shown in Fig. 17. Top: the original pulse, which was duplicated and scaled to produce the matrix of waveforms beneath. Bottom: Synthetic acoustic pulses obtained by summing pairs of original pulses with relative lags between 0.15 and 0.3 s (vertical axis) and with amplitude ratios for the first event varying from 25% to 150% of the second event (horizontal axis). (b) Comparison of example recorded (left) and synthetic (right) pulses, with applied lags and amplitude ratios as indicated. Although waveforms are not matched identically, overall resemblance is compelling. 70% of explosions examined exhibited acoustic pulses which resembled these summed waveforms, suggesting that a significant proportion of lava lake explosion signals arise from multiple or sputtering bubble bursts.

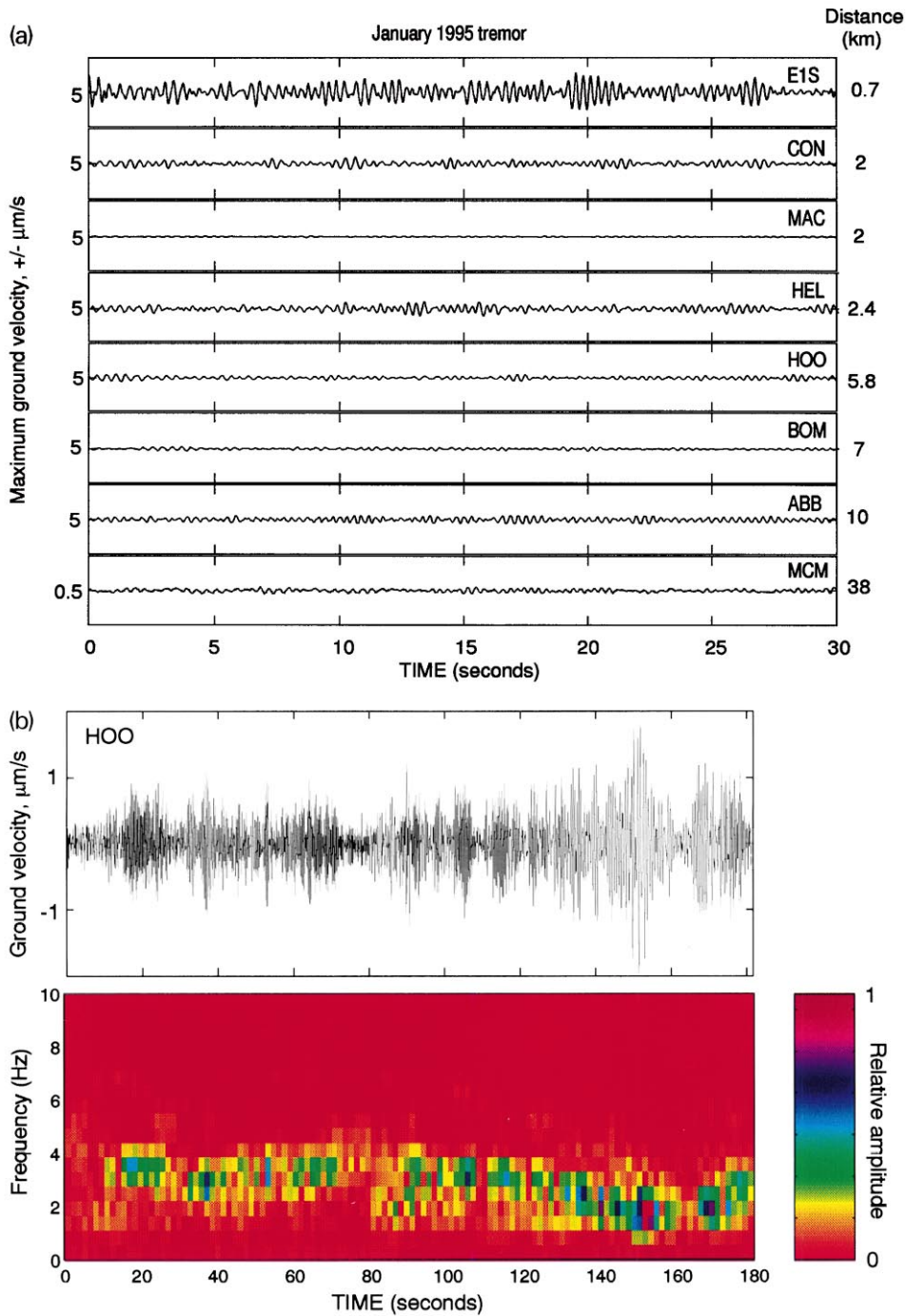


Fig. 19. Monochromatic tremor recorded by the triggered MEVO data acquisition system in January, 1995. (a) example seismograms showing 30 s of data at eight recording stations. Note that the signal is visible at McMurdo station MCM, 37 km from the conduit. Highest amplitudes were recorded at stations EIS and CON, 0.7 and 2.1 km from the lava lake, respectively, indicating a centrally located source. (b) 180 s of signal as recorded at station HOO and associated spectrogram. Horizontal axis is time (in seconds); vertical axis represents frequency (Hz). Normalized spectral amplitude is indicated by the color bar at right. The signal is strongly monochromatic at about 3 Hz, but exhibits gliding (gradual frequency decrease) of about 1 Hz around 130 s into the recording.

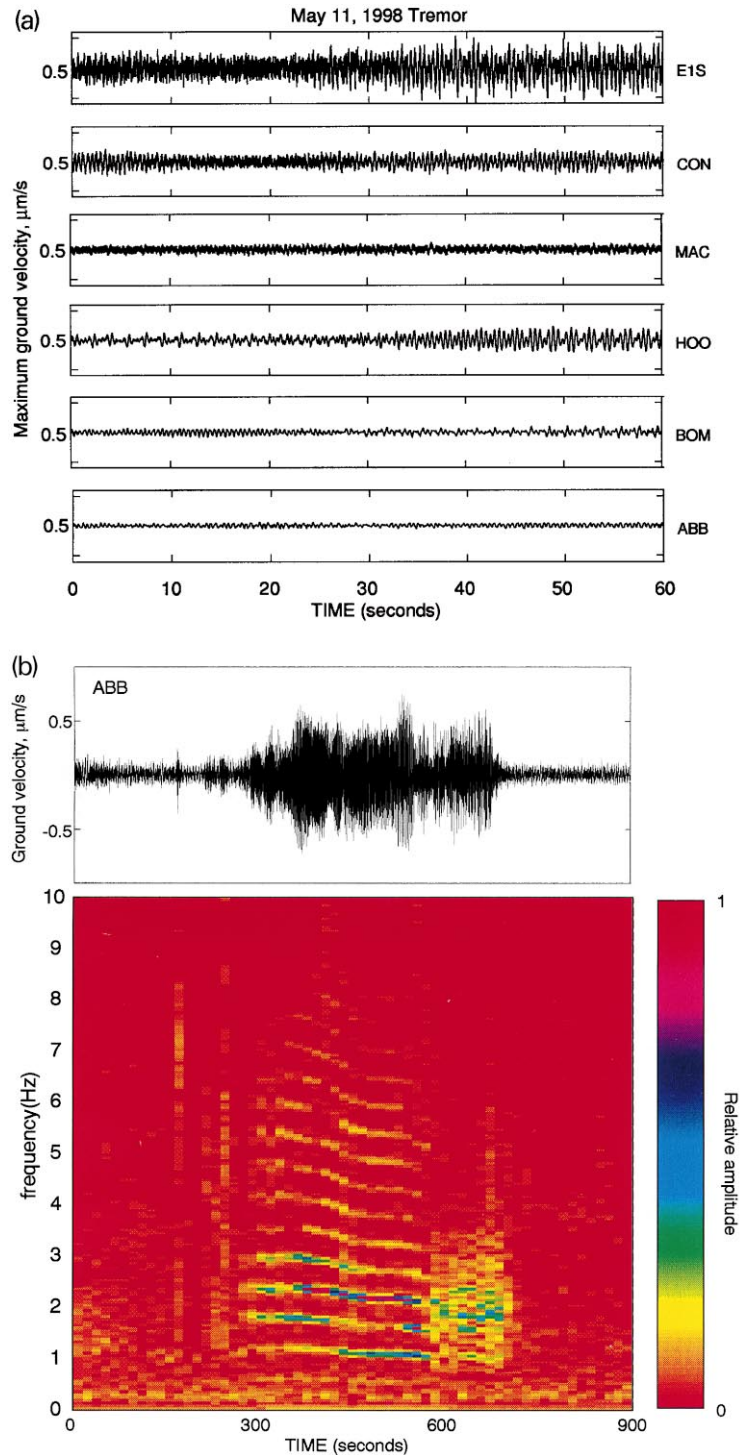


Fig. 20. Polychromatic tremor recorded on May 11, 1998. (a) Examples seismograms for a 60 s window showing the complex nature of the signal. (b) seismogram for station ABB showing 900 s of signal and associated spectrogram. Relative spectral amplitudes are indicated by the colorbar at right. Note at least twelve identifiable peaks in this short (~ 10 min) episode of tremor. Downward gliding (proportional shifting of all visible spectral peaks) of about one spectral line spacing can be clearly seen as the signal evolves.

several minutes, and particle motions project to a source centroid up to a few hundred meters beneath the lava lake surface (although this could be biased to greater depth by near-field radial tilting). These observations are consistent with a model in which large, slowly accumulating gas slugs rising to the surface explode (Chouet et al., 1998), and excite VLP resonances. Any precursory inflation was sufficiently below the passband of the instruments and/or below the site/instrumental noise to be undetectable with these data, and we conclude that recharge typically occurs with a time constant in excess of several minutes. The extended VLP signal, if it is a seismic resonance, requires very low phase velocities such as shear-coupled waves (Biot, 1952) in partial melt at the conduit wall (Rowe et al., 1998) or excitation of crack waves (Chouet, 1986; Ferrazzini and Aki, 1987). Alternatively, this signal could possibly be linked to recharge-related equilibration processes occurring in the disturbed lake following the explosion (Julian, 1994).

A sharply declining seismic/acoustic amplitude ratio for smaller explosions suggests that events exhibit systematically poorer seismic coupling with diminishing size; this may be a manifestation of stratification and acoustic isolation with the upper portion of the magma column, and/or a result of stronger attenuation within the shallow, vesiculated portion of the lake, to which the smallest explosions are presumably restricted. Acoustic and seismic waveforms frequently exhibit sub-event complexity which can be synthesized by superposition of Green's function pulses with different time lags ranging from 0.15 to 0.3 s, using a suite of amplitude ratios.

Tremor at Erebus is uncommon, with only a few isolated instances identified in the 25-year history of seismic monitoring. Most documented tremor episodes have been weak and short-lived, usually lasting only five to ten minutes, although a September 1998 example continued intermittently for two hours. Tremor signals exhibit both monochromatic and polychromatic spectra. Amplitudes are highest at stations nearest the central conduit, and exhibit lower attenuation with distance by a factor of about 5 compared to summit explosions, suggesting a source at considerably greater depth than the lava lake.

Acknowledgements

The authors would like to thank Al Eschenbacher, New Mexico Tech, for discussions regarding the December 1997 avalanche and explosion swarm; Bernard Chouet and Gilberto Saccorotti at USGS Menlo Park and Richard Lockett, British Geological Survey, for discussions and access to waveform data, and Ian Main, University of Edinburgh, for frequency–magnitude discussion. The manuscript was improved thanks to the remarks of two anonymous reviewers. McMurdo technicians Jeanne Kelley and Glenn Grant assisted greatly in network operations. This study was funded by NSF-OPP grant #9419267, with instrumental support provided by the NSF IRIS PASSCAL program.

References

- Aki, K., 1981. Deep volcanic tremor and magma ascent mechanism under Kilauea, Hawaii. *J. Geophys. Res.* 87, 7095–7109.
- Aki, K., Richards, P.G., 1980. *Quantitative Seismology, Theory and Methods*. W.H. Freeman, San Francisco, CA, pp. 485–486.
- Benoit, J.P., McNutt, S.R., 1997. New constraints on source processes of volcanic tremor at Arenal Volcano, Costa Rica, using broadband seismic data. *Geophys. Res. Lett.* 24 (4), 449–452.
- Biot, M.A., 1952. Propagation of elastic waves in a cylindrical bore containing a fluid. *J. Appl. Phys.* 23, 997–1005.
- Chouet, B.A., 1981. Ground motion in the near field of a fluid-driven crack and its interpretation in the study of shallow volcanic tremor. *J. Geophys. Res.* 86, 5985–6016.
- Chouet, B.A., 1985. Excitation of a buried magmatic pipe: a seismic source model for volcanic tremor. *J. Geophys. Res.* 90, 1881–1893.
- Chouet, B.A., 1986. Dynamics of a fluid-driven crack in three dimensions by the finite difference method. *J. Geophys. Res.* 91, 13 967–13 992.
- Chouet, B., 1996. New methods and future trends in seismological volcano monitoring. In: Scarpa, R., Tilling, R.I. (Eds.), *Monitoring and Mitigation of Volcano Hazards*. Springer, Berlin, pp. 23–97.
- Chouet, B., 1996. Long-period volcano seismicity: its source and use in eruption forecasting. *Nature* 380, 309–316.
- Chouet, B., Saccorotti, G., Martini, M., Dawson, P., De Luca, G., Milana, G., Scarpa, R., 1997. Source and path effects in the wave fields of tremor and explosions at Stromboli Volcano, Italy. *J. Geophys. Res.* 102, 15 129–15 150.
- Chouet, B., Dawson, P., DeLuca, G., Martini, M., Milana, G., Saccorotti, G., Scarpa, R., 1998. *Array Analyses of Seismic Wavefields Radiated by Eruptive Activity at Stromboli Volcano, Italy*. Gruppo Nazionale per la Vulcanologia, Italia, Litografia Felici, Pisa, Italy.

- Dibble, R.R., 1994. Velocity modelling in the erupting magma column of Mount Erebus, Antarctica. In: Kyle, P.R. (Ed.), *Volcanological and Environmental Studies of Mount Erebus, Antarctica*. Antarctic Research Series, American Geophysical Union, Washington DC, pp. 17–33.
- Dibble, R.R., Kienle, J., Kyle, P.R., Shibuya, K., 1984. Geophysical studies of Erebus volcano, Antarctica, from December to January. *N. Z. J. Geol. Geophys.* 27, 425–455.
- Dibble, R.R., Barrett, S.I.D., Kaminuma, K., Miura, S., Kienle, J., Rowe, C.A., Kyle, P.R., McIntosh, W.C., 1988. Time comparisons between video and seismic signals from explosions in the lava lake of Erebus Volcano, Antarctica. *Bull. Disaster Res. Inst. (Kyoto University, Uji, Japan)* 38, 49–63.
- Dibble, R.R., Kyle, P.R., Skov, M.J., 1994. Volcanic activity and seismicity of Mount Erebus, 1986–1994. *Antarct. J. US* 29 (5), 11–14.
- Dibble, R.R., O'Brien, B., Rowe, C.A., 1994. The velocity structure of Mount Erebus, Antarctica, and its lava lake. In: Kyle, P.R. (Ed.), *Volcanological and Environmental Studies of Mount Erebus, Antarctica*. Antarctic Research Series, American Geophysical Union, Washington, DC, pp. 1–16.
- Ferrazzini, V., Aki, K., 1987. Slow waves trapped in a fluid-filled infinite crack: Implication for volcanic tremor. *J. Geophys. Res.* 92, 9215–9223.
- Garces, M.A., Hagerty, M.T., Schwartz, S.Y., 1998. Magma acoustics and time-varying melt properties at Arenal volcano, Costa Rica. *Geophys. Res. Lett.* 25 (13), 2293–2296.
- Giggenbach, W.F., Kyle, P.R., Lyon, G.L., 1973. Present volcanic activity on Mt. Erebus, Ross Island, Antarctica. *Geology* 1, 135–156.
- Hagerty, M., Schwartz, S.Y., Protti, M., Garces, M., Dixon, T., 1997. Observations at Costa Rican volcano offer clues to causes of eruptions. *EOS Trans. Am. Geophys. Union* 78 (49), 565–571.
- Hidaya, D., Voight, B., Nyblade, A., Langston, C.A., Ratdomopurbo, A., Subandriyo, S., Ebeling, C., 1998. Broadband seismic experiment at Merapi volcano, Java, Indonesia January-February 1998: Deformation pulses embedded in multiphase and low-frequency earthquakes (abstract). *EOS Trans. Am. Geophys. Union* 79 (45), F619.
- Julian, B., 1994. Volcanic tremor: nonlinear excitation by fluid flow. *J. Geophys. Res.* 99, 11 859–11 877.
- Kaminuma, K., 1994. The seismic activity of Mount Erebus in 1981–1990. In: Kyle, P.R. (Ed.), *Volcanological and Environmental Studies of Mount Erebus, Antarctica*. Antarctic Research Series, American Geophysical Union, Washington DC, pp. 35–50.
- Kaminuma, K., Ueki, S., Kienle, J., 1985. Volcanic earthquake swarms at Mt. Erebus, Antarctica. *Tectonophysics* 114, 357–369.
- Kaneshima, S., Kawakatsu, H., Matsubayashi, H., Sudo, Y., Tsutsui, T., Ohminato, T., Ito, H., Uhira, K., Yamasato, H., Oikawa, J., Takeo, M., Iidaka, T., 1996. Mechanism of phreatic eruptions at Aso Volcano inferred from near-field broadband seismic observations. *Science* 273, 642–645.
- Kienle, J., Kyle, P.R., Estes, S., Takanami, R., Dibble, P.R., 1981. Seismicity of Mt. Erebus, 1980–81. *Antarct. J. US* 16 (5), 35–36.
- Kienle, J., Marshall, D.L., Estes, S.A., Dibble, R.R., Shibuya, K., Kyle, P.R., 1982. Seismicity of Mount Erebus, 1981–1982. *Antarct. J. US* 17 (5), 29–31.
- Kienle, J., Marshall, D.L., Kyle, P.R., Kaminuma, K., Shibuya, K., Dibble, R.R., 1983. Volcanic activity and seismicity of Mt. Erebus, 1982–83. *Antarct. J. US* 18 (5), 41–44.
- Kienle, J., Rowe, C.A., Kyle, P.R., McIntosh, W.C., Dibble, R.R., Kaminuma, K., Shibuya, K., 1985. Eruption of Mount Erebus, and Ross Island seismicity 1984–1985. *Antarct. J. US* 20 (5), 25–27.
- Knight, R.L., Dibble, R.R., Aster, R.C., Kyle, P.R., Ameko, A.K., 1996. Digital recording of the Seismicity of Mount Erebus Volcano, November 1994–June 1996. *Antarct. J. US* 31 (2), 41–43.
- Kyle, P.R. (Ed.), 1994. *Volcanological and Environmental Studies of Mount Erebus, Antarctica*. Antarctic Research Series, American Geophysical Union, Washington DC.
- Kyle, P.R., Dibble, R.R., Giggenbach, W.F., Keys, J., 1982. Volcanic activity associated with the anorthoclase phonolite lava lake, Mount Erebus, Antarctica. In: Craddock, C. (Ed.), *Antarctic Geoscience*. University of Wisconsin Press, Madison, pp. 734–745.
- Lee, W.H.K., 1992. The Xdetect program, A course on PC-based seismic networks. In: Lee, W.H.K., Dodge, D.A. (Eds.), *US Geol. Surv. Open File Rep.* 92-441, pp. 138–151.
- McNutt, S.R., 1994. Volcanic tremor from around the world: update. *Acta Vulcanol.* 5, 197–200.
- Mogi, K., 1958. Relations of the eruptions of various volcanoes and the deformations of the ground surfaces around them. *Bull. Earthquake Res. Inst. Tokyo Univ.* 36, 99–134.
- Neuberg, J., Lockett, R., Rippey, M., Braun, T., 1994. Highlight from a seismic broadband array on Stromboli volcano. *Geophys. Res. Lett.* 21, 749–752.
- Ripepe, M., Poggi, P., Braun, T., Gordeev, E., 1996. Infrasonic waves and volcanic tremor at Stromboli. *Geophys. Res. Lett.* 23 (2), 181–184.
- Rowe, C.A., 1988. Seismic velocity structure and seismicity on Mount Erebus Volcano, Ross Island, Antarctica. MS thesis, University of Alaska Fairbanks.
- Rowe, C.A., Kienle, J., 1986. Seismicity in the vicinity of Ross Island, Antarctica. *J. Geodyn.* 6, 375–385.
- Rowe, C.A., Davies, J.N., 1990. Analysis of continuous digital seismic records for the 1989–1990 Redoubt Volcano eruption (abstract). *EOS Trans. Am. Geophys. Union* 71 (43), 1709.
- Rowe, C.A., Aster, R.C., Kyle, P.R., Schlue, J.R., Dibble, R.R., 1998. Broadband recording of Strombolian explosions and associated very-long-period seismic signals on Mount Erebus volcano, Ross Island, Antarctica. *Geophys. Res. Lett.* 25 (13), 2297–2300.
- Skov, M., 1994. Digital seismic data acquisition and processing as applied to seismic networks in the Rio Grande rift and on Mount Erebus, Antarctica. MS thesis, New Mexico Institute of Mining and Technology, Socorro, NM, USA.
- Stephens, C.D., 1996. (Unpublished.) DAYPLOT, a program for generating PostScript pseudohelicorder computer plots from 24-hour, continuous digital seismic data.
- Tytgat, G., Davies, J., Rowe, C., Whitter, J., Sonafank, C., 1992.

- Example applications of continuously recorded digital data from telemetered seismographic networks for volcano and earthquake monitoring (abstract). *Seismol. Res. Lett.* 63 (1), 53.
- Ueki, S., Kaminuma, K., Baba, M., Koyama, E., Kienle, J., 1984. Seismic activity of Mount Erebus, Antarctica in 1982–1983. In: Nagata, T. (Ed.), *Proceedings of the Fourth Symposium on Antarctic Geoscience*, Tokyo, Japan, October 1983. *Memoirs of the National Institute of Polar Research, Special Issue* 33, pp. 29–40.
- Wassermann, J., 1997. Locating the sources of volcanic explosions and volcanic tremor at Stromboli volcano (Italy) using beam-forming on diffraction hyperboloids. *Phys. Earth Planet. Inter.* 104, 271–281.
- Weiss, J., 1997. The role of attenuation on acoustic emission amplitude distribution and *b*-values. *Bull. Seismol. Soc. Am* 87 (5), 1362–1367.
- Wielandt, E., Forbriger, T., 1999. Near-field seismic displacement and tilt associated with the explosive activity of Stromboli. *Ann. Geofis.* 42 (3), 407–416.